MAGNETIC FIELD INDUCED BY THERMO ELECTRIC CURRENT IN LCLS-II CRYOMODULES*

G. Wu[†] and S. K. Chandrasekaran, Fermilab, Batavia, USA

Abstract

The Seebeck effect in metals plays an important role in cryomodule design and performance. As the cryomodule is cooled from room temperature to nominal cavity operating temperature of 2 K, components in the cryomodule experience varying temperatures. Some components such as power couplers have gradients from 300 K to 2 K. Such gradients and metallic paths form thermo-electric current loops that circulate through and around the niobium cavities. These currents will generate an additional magnetic field that could be trapped in the cavity wall during superconducting transition, as well as during cavity quench. This trapped field can degrade the cavity's quality factor and increase heat load. A simple circuit model is proposed and compared to a calculated trapped field during LCLS-II cryomodule tests.

INTRODUCTION

Continuous wave (CW) cryomodules such as those in LCLS-II [1] have a high dynamic heat load. A high quality factor therefore becomes essential to reduce the demand for cryoplant capacity. Magnetic fields trapped in the niobium wall of the cavity could increase the surface resistance and increase dynamic heat load.

Residual magnetic field in a cryomodule can be attenuated by careful magnetic shield design [1], magnetic hygiene [2], and demagnetization [3]. However, as a cryomodule is cooled down, cavities in the cryomodule experience magnetic fields induced by thermo-electric currents.

There are two components of thermo-electric currents. The thermo-electric current generated during fast cool down could be quite dramatic and has been studied extensively [4-6]. The thermo-electric current related to cryomodule's materials itself is not related to fast cool down and is present regardless of cavity cool down rate. This current is generated by various cryomodule components that at different temperatures create a net thermo-electric current through cavities. Such field, if not expelled by cavities' fast cool down rate [7], could be trapped by niobium during superconducting transition and increase the dynamic heat load.

Such a field also presents a risk that the cavity could have increased dynamic head load in the event of a quench that the magnetic field can be easily trapped, until the cavity is warmed up and fast cooled. Although a large effort has been taken to ensure the cavities can expel residual magnetic field during a fast cool down, there are a few exceptions where cavities did not expel the magnetic flux as expected [7].

A better understanding of this thermo-electric current is needed to improve the design of the cryomodules.

CRYOMODULE THERMAL DESIGN

After a careful review of LCLS-II cryomodule design, we identified several thermo-electric current loops that could potentially include the cavities. Despite the cavities having two-layer magnetic shields, thermo-electric currents that flow through a cavity will induce a magnetic field within the magnetic shield, and shall therefore be witnessed by that cavity. Any thermo-electric current that does not go through cavities will have its induced magnetic field shielded by the magnetic shields.

Each cavity has a helium vessel exhaust connecting the cavity helium vessel to the 2-phase helium pipe. This exhaust, often referred to as the "chimney," has a bi-metallic joint containing titanium and stainless steel. The 2-phase helium pipe spans the entire length of the cryomodule and connects to each cavity. The 2-phase helium pipe has an additional inlet from JT valve, as well as inlets through the eight cavities supplying helium and an outlet connects to a gaseous helium return pipe. During initial cool down, there may be non-uniform temperatures among the eight helium vessel exhausts. The cryomodule cool down procedure requires the cryomodule to be warmed up to 45 K before cavities are precipitously cooled down through the superconducting transition. The procedure usually equalizes the "chimney" temperatures down to approximately 3 K, as extrapolated from cavity temperatures during the LCLS-II prototype cryomodule testing where temperature sensors read the temperatures along the string assembly. It is unlikely that this temperature gradient would result in significant thermo-electric currents.

Each cavity also has two high order mode coupler feedthroughs connected to the 2-phase pipe through copper thermal straps. The temperatures of these feedthroughs were measured in the prototype cryomodule and did not show temperature differences greater than 2 K.

The tuner motor is another device that has a thermal strap connected to 5 K pipe, while being connected to the cavity through the tuner. During cryomodule cool down, however, the tuner motors are not operated, and their temperatures remain consistent.

Thermal straps of quadruple magnet did indicate hotter temperature than the cavities. However, the magnet is relatively far away from its nearest neighboring cavity, and it is estimated that the thermo-electric loop bypasses the cavities.

Fundamental power couplers extend from the cavities at 2 K to the cryomodule's vacuum vessel at 300 K, with intermediate thermal intercepts with copper straps at 5 K and 45 K. The couplers, therefore are electrically connected to the cavities, 5 K thermal straps, 45 K thermal straps and

---

room vacuum vessel. The couplers temperatures have been measured and showed the greatest variations.
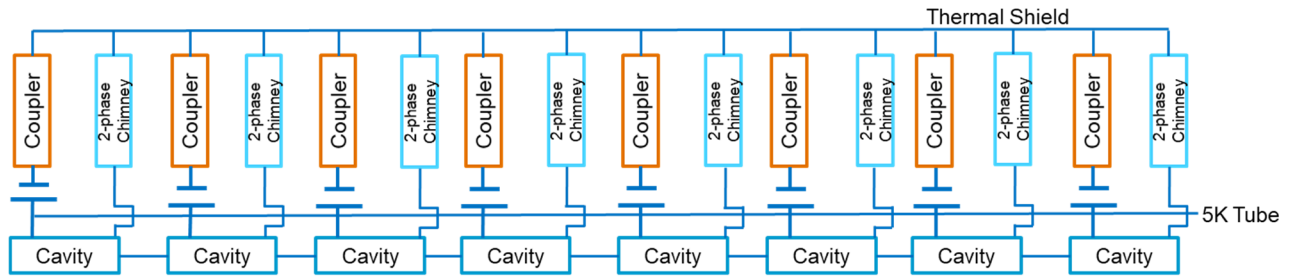
Figure 1: An illustration of circuit model of couplers and cavities connected to 5 K tube and 45 K thermal shield.

Among those mentioned above, the coupler thermo-electric loops are considered the most probable cause of the residual magnetic field, due to the largest thermal gradient across each coupler. There are other electric loops that could potentially have thermo-electric current. If the current does not flow through cavities, however, the induced magnetic field is negligible compared to earth magnetic field and are attenuated by magnetic shield.

COUPLER THERMO-ELECTRIC LOOP

The Seebeck voltages in the thermo-electric loops illustrated in Figure 1 could be different for each coupler, therefore generating currents through the cavities.

The steady state temperature profile across a coupler within the LCLS-II cryomodule is illustrated in Figure 2. Parts in the figure include a coupler antenna connected to room temperature waveguide (not shown), coupler outer is connected to 2 K coupler port on a cavity, a 5 K thermal strap connected couplers thermal intercept and 5 K helium pipe, coupler's 45 K thermal intercept connected to cryomodule's thermal shield which ranges from 35 K to 55 K depending on the location of the cavity position.
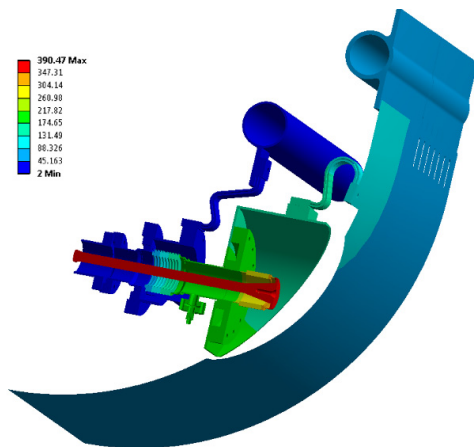
Figure 2: A static temperature profile of LCLS-II power coupler in a sectional view.

MAGNETIC FIELDS OF THERMOELEC-TRIC CURRENTS

The magnetic fields measured within the cavities' helium vessels of the prototype cryomodule are illustrated in

Figure 3, in comparison to the temperature of cavity 1. This was a slow cool down, where the cavity temperature was very uniform in various locations including HOM coupler bodies, beam pipes and cavity cell 1 and cell 9. This slow cool down demonstrates that the increases in the magnitude of magnetic field was caused only by the cryomodule components and not the cavity temperature variation that is present during a fast cool down.
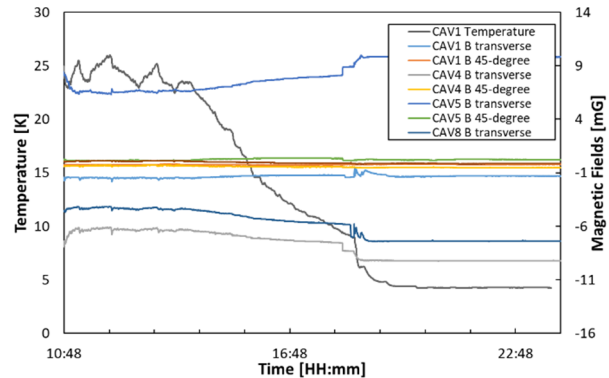
Figure 3: Magnetometer readings during slow cool down.

The variation of the coupler temperatures in comparison to the temperature of cavity 1 is illustrated in Figure 4. For the prototype cryomodule, the coupler thermal strap installation procedure and locations were not yet optimized. Coupler 45 K thermal anchors showed a maximum of 13 K difference between coupler of cavity 5 and coupler of cavity 8.
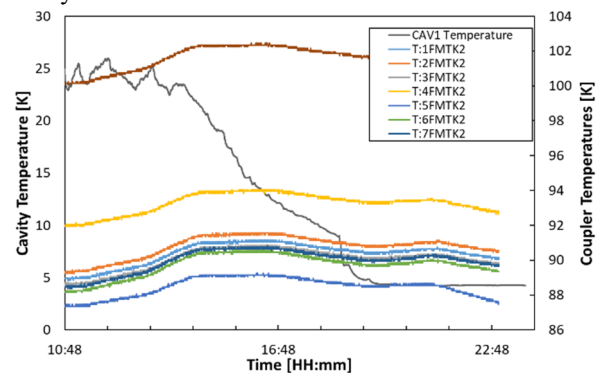
Figure 4: Coupler temperatures during slow cool down.

An extrapolated Seebeck coefficient for iron was used for stainless steel [8]. The resistance is mostly dominated

by contact resistance between thermal straps. A temperature difference of 13 K between couplers was approximately in the order of 5 mG. This was close to what was measured in prototype cryomodule.

For production cryomodules, there were no magnetic field measurements from within the cavity helium vessels. Nevertheless, cavity slow cool downs were conducted for the production cryomodules. Cavity quality factors were measured, and the trapped field was estimated using previously measured surface resistance to the magnetic field ratio of 1.4 nΩ/mG. Such estimated magnetic fields for several production cryomodules are illustrated in Figure 5. Note that each cryomodule has 8 cavities, and therefore cavities 1—8 are in the prototype cryomodule 1, 9—16 are in production cryomodule 2, and so forth.
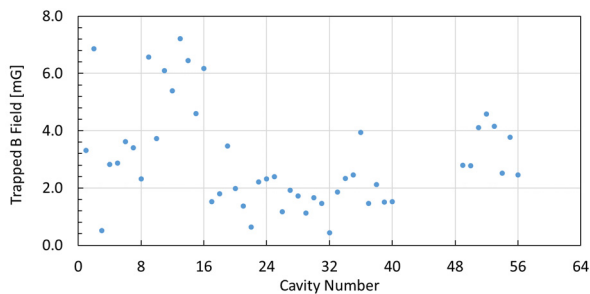
Figure 5: Cavity trapped magnetic field for cryomodules. Each module has 8 cavities.

Table 1 lists the trapped magnetic field estimated using Q_0 measurement. Each coupler had two temperature sensors measuring 45 K flanges. Temperature **T** in the table was the average of all eight couplers. **ΔT** was the temperature difference between the hottest and coldest, providing the greatest differential.

Table 1: Coupler temperatures and estimated trapped magnetic fields. **T** is the average temperature of the couplers in the cryomodule, and **ΔT** is the difference between the coldest and hottest couplers for that cryomodule.

Cryomodules	T [K]	ΔT [K]	B [mG]
F1.3-01 (pCM)	95	7	3.2
F1.3-04	68	3	1.5
F1.3-07	81	8	3.4

DISCUSSION

The electric circuit of a cryomodule is very complex. The data analysis presented here was a first order estimate of a primary cause of increased magnetic fields when the cryomodule was cold. The coupler temperatures at the 45 K thermal intercepts varied from cavity to cavity in a cryomodule. The data showed some likely correlation between the coupler temperature variation and thermoelectric current induced magnetic fields.

During LCLS-II cryomodule production thermal straps were improved continuously. After the Fermilab prototype cryomodule was tested, cold ends of 45 K thermal straps were relocated from lower part of the cryomodule thermal shield to upper portion where is it much closer to the 45 K

helium flow. Starting from CM04, 45 K thermal strap connections started to use indium foil as well to reduce contact resistance and improve reliability.

The cryomodule test procedure was also improved to increase the 45 K flow rate to reduce the coupler temperatures at the 45 K intercepts. Once the cavities in a cryomodule completes the superconducting transition, 45 K flow can be restored to operating settings.

Unfortunately, a shortened production cryomodule test plan eliminated the slow cool down cycle. There was not enough data to show how the thermoelectric current induced field was improved for the remaining production cryomodules.

CONCLUSION

A large effort has been taken to design the best magnetic shield, implement the best magnetic hygiene practices, and conduct cryomodule demagnetization. Yet, thermo-electric currents increase the residual magnetic field. Fast cool down does expel those residual fields but does not help during cavity quench. In addition, the presence of this thermo-electric current induced magnetic fields burdens the cavity material selection and post processing to improve and rely on flux expulsion.

CW cryomodules could benefit greatly if thermoelectric current can be minimized during cool down. This is especially important for future film-based CW cryomodules, such as those with niobium coated on copper and Nb3Sn cavities, which cannot be fast cooled due to thermo-electric currents generated between the film and the parent material.

More tests and developments are planned for future cryomodules at Fermilab, such as the cryomodules for the PIP-II project.

ACKNOWLEDGEMENT

REFERENCES

[1] T. J. Peterson et al., "LCLS-II 1.3 GHz Cryomodule Design Modified TESLA-Style Cryomodule for CW Operation", in *Proc. SRF'15*, Whistler, Canada, Sep. 2015, paper THPB119, pp. 1417-1421.
doi: 10.18429/JACoW-SRF2015-THB119

[2] G. Wu, "Overview on Magnetic Field Management and Shielding in High Q Modules", in *Proc. SRF'15*, Whistler, Canada, Sep. 2015, paper THBA06, pp. 1043-1048.
doi: 10.18429/JACoW-SRF2015-THBA06

[3] S. K. Chandrasekaran and A. C. Crawford, "Demagnetization of a Complete Superconducting Radiofrequency Cryomodule: Theory and Practice," in *IEEE Transactions on Applied Superconductivity*, vol. 27, no. 1, pp. 1-6, Jan. 2017.

[4] J. M. Vogt, O. Kugeler, J. Knobloch, "High-Q Operation of SRF cavities: The Potential Impact of Thermocurrents on the rf Surface Resistance", in *arXiv preprint arXiv:1503.00601*, 2015 - arxiv.org.

[5] V. Cooley, "Study of Thermocurrents in ILC Cavities via Measurements of the Seebeck Effect in Niobium, Titanium,

and Stainless Steel Thermocouples", 2014. Web. doi:10.2172/1331105.

[6] G Wu, A Grassellino, E Harms, N Solyak, A Romanenko, C Ginsburg, R Stanek, "Achievement of Ultra-High Quality Factor in Prototype Cryomodule for LCLS-II", in *arXiv preprint arXiv:1812.09368,* 2018 - arxiv.org.

[7] S Posen, et al., "Role of magnetic flux expulsion to reach $Q_0 > 3 \times 10^{10}$ in superconducting rf cryomodules", in *Phys. Rev. Accel. Beams, vol.* 22, p. 032001, 2019.

[8] W. Fulkerson, J. P. Moore, and D. L. McElroy, " Comparison of the Thermal Conductivity, Electrical Resistivity, and Seebeck Coefficient of a High-Purity Iron and an Armco Iron to 1000°C ", in *J. App. Phys.,* vol. 37, p. 2639, 1966.